Proceedings of the 5th International Symposium on Steel Science (ISSS 2017)
Nov. 13-16, 2017, Kyoto, Japan: The Iron and Steel Institute of Japan

Grain boundary character analysis by correlative transmission electron microscopy / atom probe tomography

Carlos Parra[1,2*], Michael Herbig[1], Dierk Raabe[1]

[1]Max-Planck-Institut für Eisenforschung GmbH, Düsseldorf, Germany

[2]Escuela Superior Politécnica Litoral, Guayaquil, Ecuador

Abstract: Many macroscopic material properties are strongly affected by grain boundary segregation. In steels, in particular carbon segregation to interfaces in austenite and ferrite is of importance. Segregation depends on the five macroscopic crystallographic parameters of the grain boundary. In prior work we have shown on a correlative transmission electron microscopy / atom probe tomography dataset how C segregation to ferritic grain boundaries depends on the disorientation angle. We currently extend this analysis by additionally considering the grain boundary plane orientation of low angle grain boundaries. Here we describe a method to identify pure low angle tilt and twist boundaries. In future this will allow measuring the carbon content per dislocation line length of edge and screw dislocations.

1. INTRODUCTION

Polycrystalline materials consist of regions with periodically arranged atoms (grains). They are separated by grain boundaries (GBs) which form an interconnected three-dimensional network. The physical properties of grain boundaries will thus affect a material's bulk performance. At GBs two differently oriented periodic atomic arrangements meet causing local structural disorder. For low angles below 15° this misfit is accommodated by dislocation arrays which can attract solute atoms particularly to their cores. The segregation of solutes generates pronounced changes in the local chemical composition. The local enrichment of hydrogen or phosphorus at interfaces can for example lead to a loss of fracture toughness [1, 2]. Equilibrium segregation of solute atoms to GBs can be described by the Gibbs adsorption isotherm. The interfacial solute excess Γ (atoms/nm^2) is a function of temperature, pressure, composition and crystallographic character of the GB. While the first three variables can be controlled, the grain boundary character is mainly a result of the system and the material processing. The GB character is defined by 5 crystallographic parameters, which are the rotation axis and angle (3 independent parameters), and the GB plane normal (2 independent parameters) plus three atomic relaxation parameters. As the latter ones can be considered to be a function of the five crystallographic parameters, these will be neglected in the following [3].

A newly developed approach for correlative atom probe tomography (APT) / transmission electron microscopy (TEM) [4, 5] enabled the measurement of 121 grain boundaries in heavily deformed pearlite wire [6] where the deformation driven cementite decomposition supplied an enhanced solute carbon content. Up to now, mainly the correlation between carbon GB segregation and the disorientation angle ω (one out of five crystallographic parameters) was investigated. A trend of increasing segregation with increasing disorientation angle was observed in the low angle grain boundary regime (ω<15°). This is because in a first order approximation the disorientation angle of a low angle grain boundary is proportional to the planar dislocation density in the interface. However, the observation of a large distribution of different C excess values, far beyond the measurement error, for the same angle ω shows that segregation in this regime is also affected by the exact buildup of the dislocation array comprising the interface. A symmetric tilt low angle boundary which is comprised of edge dislocations only can be expected to attract different amounts of solutes than a symmetric twist low angle GB which is primarily composed of screw dislocations, even if both have the same disorientation angle [7]. In order to understand the consequence of such effects on carbon solubility, we establish a procedure that allows to identify tilt and twist grain boundary portions as only for those the dislocation arrangement can be uniquely identified based on the five crystallographic boundary parameters.

* Corresponding Author. E-mail: cparra@espol.edu.ec, telephone: +593 93-992-8346.

The following steps were conducted consecutively to perform this analysis: The information gathered with the different characterization techniques were merged into the same coordinate system (were registered). Grain orientations obtained from nanobeam diffraction (NBD) were used to calculate all crystallographically equivalent solutions for misorientation angle/axis pairs by considering the symmetry operators of the crystal system. The grain boundary normal was extracted from scanning TEM (STEM) micrographs, the sign of the boundary inclination was extracted from 3D atom probe datasets. With that having determined the five crystallographic boundary parameters, the GB character was determined: The tilt and twist character of the boundaries was identified, by calculating the angle between GB normal $\vec{n}$ and the rotation axis. This manuscript summarizes the data processing steps required to conduct this procedure.

2. MATERIAL AND EXPERIMENTAL METHODS

The analysis was performed on pearlitic wires with a composition of 4.40C, 0.30Mn, 0.39Si and 0.21Cr (at. %). Samples were cold drawn ($\varepsilon = 6$) and subsequently subjected to annealing for 2 minutes at 400˚C, to generate a microstructure consisting of columnar ferritic grains, separated by grain boundaries which are covered by carbon GB segregation. The atom probe samples were prepared by focus ion beam (FIB) milling in such way, that their resulting main axis was perpendicular to that of the columnar grains. Transmission electron microscopy was performed on the atom probe samples with the electron beam parallel to the main axis of the columnar grains, thereby avoiding grain overlaps. The grains had a diameter of approximately 30 nm. The data set processed in this work was comprised of STEM micrographs, NBD patterns (acquired in both, scanning and spot mode), and 3D atom maps measured by APT, containing information on the grain boundary plane, grain orientations and local chemical compositions, respectively.

3. REGISTRATION OF THE DATA SETS

APT and TEM are two complementary techniques. While chemical information (Γ) was obtained from APT, the crystallographic information was obtained from TEM techniques. The output of the three TEM techniques employed (STEM imaging, NBD in STEM spot mode and NBD in scanning mode) was rotated about the incident beam axis in TEM with respect to each other (magnetic rotation) which had to be compensated for. Magnetic rotation occurs due to the precession of the electrons about their center axis in the TEM and varies with the instrument settings, such as the camera length. In the current case the calibration of the magnetic rotation was conducted using a perfectly coherent twin boundary. The grain orientations as received from NBD were given in the Euler angles φ_1, Φ, and φ_2, following the Bunge convention. Since the magnetic rotation χ only causes a rotation about the incident beam, it only needed to be added to the first Euler angle, φ_1, of the grain orientations. Eqs. 1 to 4 describe the compensation of the magnetic rotation and the conversion of the grain orientations from Euler angles into 3x3 orientation matrices. $g_{\varphi 1}$, g_{Φ}, and $g_{\varphi 2}$ are intermediate rotation matrices and g is the final grain orientation matrix in <100> row vectors. From now on all orientation calculations were conducted using 3x3 matrices.

$$g_{\varphi 1} = \begin{pmatrix} \cos(\varphi_1 + \chi) & \sin(\varphi_1 + \chi) & 0 \\ -\sin(\varphi_1 + \chi) & \cos(\varphi_1 + \chi) & 0 \\ 0 & 0 & 1 \end{pmatrix} \quad (1)$$

$$g_{\Phi} = \begin{pmatrix} 1 & 0 & 0 \\ 0 & \cos\Phi & \sin\Phi \\ 0 & -\sin\Phi & \cos\Phi \end{pmatrix} \quad (2)$$

$$g_{\varphi 2} = \begin{pmatrix} \cos\varphi_2 & \sin\varphi_2 & 0 \\ -\sin\varphi_2 & \cos\varphi_2 & 0 \\ 0 & 0 & 1 \end{pmatrix} \quad (3)$$

$$g = g_{\varphi 2} \cdot g_{\Phi} \cdot g_{\varphi 1} \tag{4}$$

4. CALCULATION OF MISORIENTATION ANGLE/AXIS PAIRS

The crystal and the specimen coordinate systems are related by a rotation matrix, just as the orientations of two abutting grains comprising a grain boundary. However, the specification of the crystal coordinate system in the cubic system is not unique and a number of different rotation matrices exist, which all convert one given cubic grain orientation into another given one. In order to calculate all equivalent solutions for the misorientation matrix the orientation matrices of each of the two adjacent grains comprising a boundary were pre-multiplied with the 24 symmetry operator matrices in the cubic system. The 24 symmetry operators in the cubic system are comprised of 2 rotations of 120˚about each of the four <111> poles, 3 rotations of 90˚about each of the three <100> poles, one rotation of 180˚about each of the six <110> poles, and the identity matrix [6]. When considering that a rotation about an axis can be conducted both in the positive and negative sense, this results in 1152 (24x24x2) symmetrically equivalent solutions describing the misorientation of a single GB. The calculation of these 1152 possible misorientation matrices Δg_{AB} is described in Eq. 5:

$$\Delta g_{AB} = (g_i * g_B) * (g_j * g_A)^{-1} = \begin{pmatrix} m_{11} & m_{12} & m_{13} \\ m_{21} & m_{22} & m_{23} \\ m_{31} & m_{32} & m_{33} \end{pmatrix} \tag{5}$$

Where g_A and g_B are the orientation matrices of the two grains (A and B) participating in the interface, as calculated from Eq. 4, g_i and g_j are the symmetry operator matrices in the cubic system of grains A and B, respectively, where i and j vary from 1, 2…24. The 1152 equivalent misorientation matrices of each grain boundary were then converted to an angle/axis representation using Eqs. 6 and 7 [8]. These symmetric equivalent misorientation angle/axis pairs were finally reduced to 12 by selecting those with the lowest misorientation angle (also referred to as disorientation angle) in the right-hand convention.

$$\omega = \cos^{-1}[(m_{11} + m_{22} + m_{33} - 1)/2] \tag{6}$$

$$\vec{O}c_{ij} = \begin{pmatrix} m_{23} - m_{32} \\ m_{31} - m_{13} \\ m_{12} - m_{21} \end{pmatrix} \tag{7}$$

Where $m_{11...}m_{33}$ represent the elements of the 3x3 misorientation matrix of each grain boundary as defined in equation 5, ω is the misorientation angle and $\vec{O}c_{ij}$ is the misorientation axis in the crystallographic coordinate system. We distinguish between crystallographic and sample coordinate system, which consider orientations with respect to a specific grain or within the reference frame of the sample, respectively.

5. DETERMINATION OF THE GRAIN BOUNDARY NORMAL

The grain boundary plane orientation is described by its normal $\vec{n}$. It was determined from BF-STEM images using the approach described in Fig. 1. Grain boundaries parallel to the electron beam in TEM are visible as single lines projected in the micrograph, as shown in Fig. 1(a) on the example of a boundary between grain 1 and 2 (G1/G2). In this case the plane orientation can be determined directly by measuring the azimuth angle in the sample coordinate system. On the other hand, inclined grain boundaries appear as two parallel lines as seen in the case of boundary G3/G4, shown in Fig. 1(a).

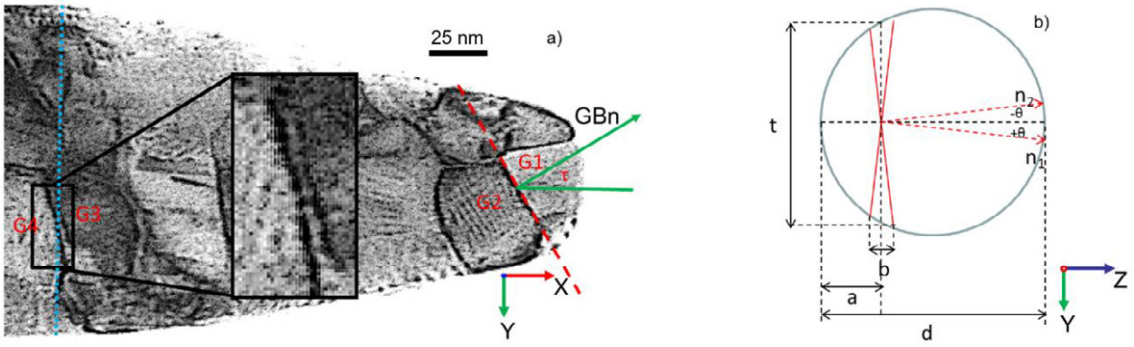

Figure 1. Determination of $\vec{n}$ from STEM micrographs. a) For a grain boundary oriented edge-on with respect to the incident beam in TEM (see G1/G2) only the azimuth angle τ needs to be calculated and the inclination angle remains zero. For a grain boundary that is inclined with respect to the incident beam (see G3/G4) the calculation of the inclination angle θ requires considering the local thickness t and the local sample diameter d (b). b) Shows is a schematic representation of a cross section through the sample at grain boundary G3/G4 as marked with a vertical dashed line in a).

These two lines are the projected intersections of the boundary with the upper and lower sample surface. In this case, the calculation of $\vec{n}$ requires besides the azimuth angle τ also taking the inclination angle θ into account. For this, the distance between the traces b and the local sample thickness t must be known. The latter one is in case of the conical APT specimens a function of the local sample diameter d, see Fig. 1(b). The local sample width at a certain point, observed in the TEM micrograph, is also the local sample diameter. The distance between traces can be directly measured from the micrograph and scaled accordingly. Finally, the local thickness varies depending on the distance of the point of interest from the center axis of the atom probe sample according to Eq. 8. The GB inclination angle was calculated using Eq. 9

$$t = 2\sqrt{\left(\frac{d}{2}\right)^2 - \left(\frac{d}{2} - a\right)^2} \tag{8}$$

$$\theta = \pm\text{atan}\left(\frac{b}{t}\right) \tag{9}$$

Where a is the distance from the center of the two parallel lines to the sample perimeter at the corresponding local sample diameter d, Fig. 1(b). This method results in two possible inclination angles with the same magnitude but different sign. The 3D atom probe reconstructions were used to determine which of these possible GB plane inclinations is correct. Finally, $\vec{n}$ under the sample coordinate system was calculated from the corresponding azimuth and elevation angles using Eq. 10.

$$\vec{n} = \begin{pmatrix} \cos\theta \cdot \cos\tau \\ \cos\theta \cdot \sin\tau \\ \sin\theta \end{pmatrix} \tag{10}$$

6. IDENTIFICATION OF TILT AND TWIST LOW ANGLE BOUNDARIES

All boundaries with disorientation angles below 15° were considered as low angle GBs. From this selection of interfaces, the tilt and twist character were determined. Boundaries with pure tilt or twist character have an angle of 90° or 0°, respectively, between disorientation axis and boundary normal. The disorientation axes as calculated using Eq. 7 are defined with respect to the reference frame of a given grain (are within the crystallographic coordinate system) while $\vec{n}$ is defined in the sample coordinate system of the specimen. To do this calculation one of them has to be transformed into the other coordinate system. Here, we transform the disorientation axes into the sample coordinate system using Eq. 11:

$$\vec{O}s_{ij} = (g_i \cdot g_A)^{-1} \cdot \vec{O}c_{ij} \tag{11}$$

Where $\vec{O}c_{ij}$ are the 12 symmetrically equivalent disorientation axes in the crystallographic coordinate system and $\vec{O}s_{ij}$ are these axes within the sample coordinate system. For this calculation g_A can be replaced by g_B; the result is the same as $\vec{O}c_{ij}$ describes a crystallographic pole which both grains of the interface have in common. Further, all 12 variants of $\vec{O}c_{ij}$ are found to yield the same disorientation axis $\vec{O}s$ in physical space. Thus, per interface there is only one GB normal and one disorientation axis in the sample coordinate system so that there is a unique solution for the angle between these vectors (α) which describes the interfaces' tilt and twist character, as calculated using Eq. 12.

$$\alpha = \arccos(\vec{n} \cdot \vec{O}s) \tag{12}$$

The accuracy of α depends mainly on two factors, the accuracy and precision of the disorientation axis which was determined using NBD and of $\vec{n}$ determined by STEM imaging. The angular resolution of NBD is typically ≤1°[9]. The second error is hard to estimate but should considering the spatial resolution of STEM imaging for straight interfaces also not exceed 1°. A cut-off value of ±3° therefore seems appropriate to identify boundaries with "pure" tilt or twist character. Thus, all boundaries with $\alpha = 90° \pm 3°$ or $\alpha = 0° \pm 3°$ were classified as pure tilt or twist boundaries, respectively.

7. CONCLUSIONS

Within the dataset of 121 GBs 32 were identified as low angle GBs. 5 of them fulfilled the above-mentioned criteria and were considered as pure tilt boundaries. The rest consisted of mixed character GBs. Due to the pronounced texture of the material no pure twist boundaries were detected. Fig. 2 depicts the dependence of the C excess on the misorientation angle for all low angle GBs in the dataset. Pure tilt GBs are marked in red, together with their corresponding angle α which describes their deviation from the ideal tilt character. A general trend is observed that the pure tilt low angle GBs give rise to less solute segregation than the average low angle GB. However, there is one escapee around $\omega = 8.5°$ that attracts far more C than the average low angle GB. This might be explained by the degree of symmetry of the tilt low angle GBs, which was not taken into account in this study. A symmetric low angle tilt boundary is composed of a single array of edge dislocations while the asymmetric one is composed of two arrays of dislocations with mutually perpendicular Burgers vectors. Further analysis concerning the dependence of C solute segregation on the symmetry angle of low angle tilt GBs will be carried out in future.